

Transformation of a Strongly Nonlinear Wave in a Shallow-Water Basin

E. N. Pelinovsky^{a, b} and A. A. Rodin^{b, c}

^a *Institute of Applied Physics, Russian Academy of Sciences, ul. Ul'yanova 46, Nizhni Novgorod, 603950 Russia*
e-mail: pelinovsky@hydro.appl.sci-nnov.ru

^b *Nizhni Novgorod State Technical University, ul. Minina 24, Nizhni Novgorod, 603950 Russia*
e-mail: xmrarro@gmail.com

^c *Institute of Cybernetics, Tallinn University of Technology, Estonia*

Received February 2, 2011; in final form, March 17, 2011

Abstract—The transformation of a nonlinear wave in shallow water is investigated analytically and numerically within the framework of long-wave theory. It is shown that the nonlinearity parameter (the Mach number), which is defined as the ratio of the particle velocity in the wave to the propagation velocity, can be well above unity in a deep trough and that a jump appears initially in the trough. It is demonstrated that shock-wave amplitudes at large times change in accordance with the prediction of weakly nonlinear theory. The shock front generates a reflected wave, which, in turn, transforms into a shock wave if the initial amplitude is large enough. The amplitude of the reflected wave is proportional to the cube of the initial amplitude (as predicted by weakly nonlinear theory) over a wide range of amplitudes except for the case of anomalously strong nonlinearity. When there is a sign-variable sufficiently intense initial perturbation, the basic wave transforms into a positive shock pulse (crest) and the reflected wave turns into a negative pulse (trough).

Keywords: water waves, nonlinear theory, shallow water, analytical and numerical solutions.

DOI: 10.1134/S0001433812020089

The process of the nonlinear transformation of a wave in shallow water is well known and admits an exact analytical description in the form of the Riemann wave within the framework of nonlinear shallow-water theory [1, 2, 5, 7, 10, 11, 17]. In this case, the emphasis is on the wave shape, its spectrum, and the time of its breaking (identified with a so-called gradient catastrophe in the framework of hyperbolic shallow-water equations). The wave collapse usually occurs near the shore or when the wave enters a river mouth [7, 8, 12, 15–18]. The motion of the breaking wave (bore) is well known; the theory usually deals with a developed bore (flow velocities on both sides of the jump approach constant values). Different types of shock waves occur depending on the height of a bore: a parabolic wave at $H > 9h$ (H is the height of the bore and h is the water depth in front of the bore), a hydraulic jump at $9h > H > 1.5h$ (the classical form of a shock wave), and an undular bore at $H < 1.5h$ [6, 7]. In the latter case, for a description of the structure of the shock wave, the dispersion effects must be taken into account (for example, in the framework of the Korteweg–de Vries–Burgers equation), and shallow-water equations in divergent form with corresponding boundary conditions at discontinuity should be considered in the first two cases. At the same time, if the wave is long enough so that the shock front occupies a

small part of the wave, it can be described in general as a shock wave by ignoring the front structure and approximating the front by a discontinuity. The change in the amplitude of the bore depends on the pattern of the wave field behind discontinuity. For a small-amplitude bore, the field outside discontinuity is still described by a solution in the form of the Riemann wave and the bore amplitude can be found analytically [7]. Here we have a full analogy with problems of nonlinear acoustics [9], where the formation and development of a shock wave in the second order of nonlinearity are analyzed in detail. However, as noted in [9], the shock wave is not inscribed in the shock-wave profile in the third order of nonlinearity and the generation of waves reflected from discontinuity is possible. This effect was experimentally observed in transmission lines for electromagnetic waves, where the dispersion effects, however, are significant [3]. For water waves, the nonlinearity can be arbitrarily strong at shallow depths; therefore, the asymptotic estimates within the framework of the weak nonlinearity approximation are not always applicable. Here, we analyze the process of formation and evolution of the shock wave in shallow water without restrictions on its amplitude within the framework of shallow-water theory.

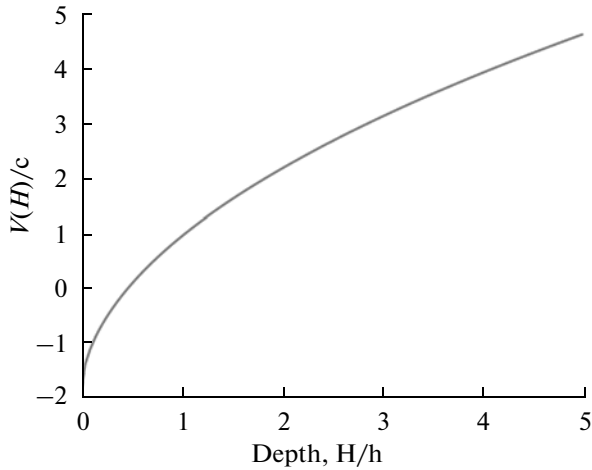


Fig. 1. Wave deformation velocity versus the local depth in the wave.

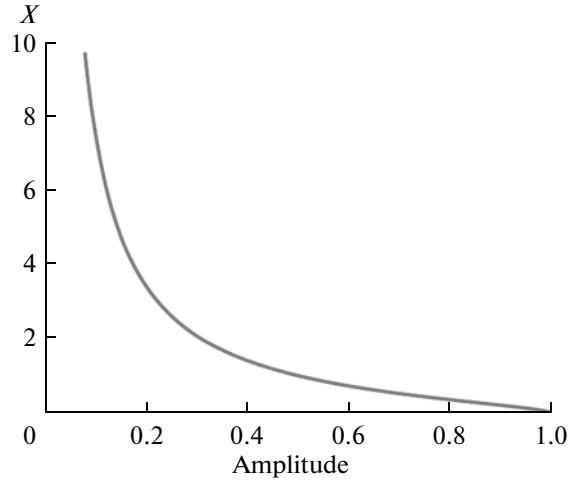


Fig. 2. Breaking length of the Riemann wave versus its amplitude.

The basic equations of the nonlinear theory of shallow water are

$$\frac{\partial u}{\partial t} + u \frac{\partial u}{\partial x} + g \frac{\partial H}{\partial x} = 0, \quad \frac{\partial H}{\partial t} + \frac{\partial}{\partial x} [Hu] = 0, \quad (1)$$

where $H(x, t) = h + \eta(x, t)$ is the water depth counted from the bottom, $\eta(x, t)$ is the water-surface displacement, u is the horizontal velocity of the water flow, g is the acceleration due to gravity, and h is the unperturbed basin depth assumed to be constant. For the waves moving in one direction (for definiteness toward $x > 0$), the order of (1) can be lowered and the equation can be written as [2, 5]

$$\frac{\partial H}{\partial t} + V(H) \frac{\partial H}{\partial x} = 0, \quad u = 2(\sqrt{gH} - \sqrt{gh}), \quad (2)$$

$$V = \sqrt{gh} + \frac{3u}{2} = 3\sqrt{gH} - 2\sqrt{gh}. \quad (3)$$

It is significant to emphasize that Eq. (2) is exact in the framework of the shallow-water theory and is valid for a wave of any amplitude up to its breaking. The general solution of (2) has the form

$$H(x, t) = H_0[x - V(H)t], \quad (4)$$

where $H_0(x)$ determines the water-surface profile at the initial time. The implicit form of (4) describes the so-called Riemann wave, which is well known in nonlinear acoustics [4, 9]. For water waves, solution (4) describes the nonlinear deformation of the wave with a steep front on its face slope. A detailed analysis of the nonlinear deformation of a shallow-water wave and of the change in its spectrum up to the collapse moment was performed in [5].

The dependence of the local propagation velocity of the wave on its amplitude, which determines the

nonlinear deformation of the wave, is shown in Fig. 1 (here $c = \sqrt{gh}$ is the celerity of linear long waves).

The velocity of a positive perturbation (wave crest) always exceeds the linear propagation velocity so that the crest acquires a steep front with time. If the wave is of negative polarity (trough), its velocity is lower than the linear velocity and a steep front forms on the back slope of the wave. If the trough is very deep so that

$$H < H_{cr} = \frac{4}{9}h, \quad (5)$$

the trough velocity becomes negative (see (3)). In this case, different portions of the wave profile propagate in different directions so that the shock wave is formed almost instantaneously. It is already seen from here that the nonlinear effects should be more pronounced in the wave trough than in its crest. Formally the nonlinearity parameter, defined as the ratio of the particle velocity in water to the wave propagation velocity (the Mach number u/V), becomes infinite. It is this case that we analyze in detail below.

The initial condition for the Riemann wave in the first series of experiments was the Gaussian pulse of negative polarity (a trough on the water surface)

$$H_0(x) = h \left[1 - A_0 \exp\left(-\frac{x^2}{l^2}\right) \right], \quad (6)$$

in which the flow velocity is defined by the right-hand side of (2) so that the wave propagated in one direction. In further calculations the unperturbed depth of a basin was set equal to $h = 1$ m and the characteristic half-size of the pulse was taken to be $l = 142$ m, so that the long-wave approximation was valid. The wave amplitude A_0 was varied widely. To take into account shock waves, the equation for the velocity on the left-hand side of (1) was replaced by the equation for dis-

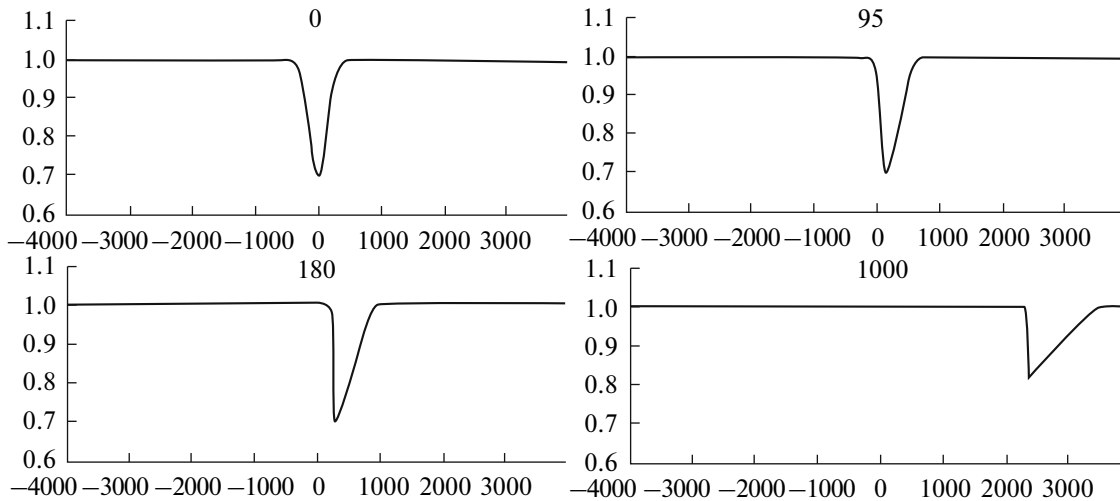


Fig. 3. Formation of a small-amplitude shock wave ($A_0 = 0.3$). The distance (in m) is on the horizontal axis, and the depth (in m) counted from the bottom is on the vertical axis. Time in seconds is shown by numbers.

charge uH to provide the divergent form of the conservation laws [13], but the equation for the water depth remained the same. Numerical calculations were carried out with the use of the Clawpack software package, which solves the hyperbolic equations using the finite-element method [13, 14]. Shallow-water equations were solved with periodic boundary conditions; the domain size was set equal to 8000 m so as to observe the nonlinear deformation of the wave. The spatial step was 8 m; its two- or threefold variation resulted in a change in wave amplitudes of no more than 1.5%. The time step is chosen to satisfy the Courant condition and is equal to 1 s.

At first, we estimate the breaking time when the Riemann wave (4) ceases to be smooth. The time of formation of the first steep portion on the wave (breaking) can be calculated exactly for any amplitude [5]

$$T_{br} = \frac{1}{\max \left[-\frac{dV}{dH} \frac{dH_0(x)}{dx} \right]}. \quad (7)$$

In particular, for the initial perturbation given by (6), the dependence of the dimensionless breaking length ($X = cT_{br}/l$) on the dimensionless wave amplitude A_0 is determined by a parametric curve

$$X = \frac{2}{3A_0} \left[y \exp(y^2) \right], \quad A_0 = (1 - 2y^2) \exp(y^2), \quad (8)$$

this dependence is shown in Fig. 2. As one might expect, the small-amplitude wave breaks at long distances (proportional to A_0^{-1}), while the large-amplitude wave breaks almost instantaneously. Note that the critical depth (5), for which $A_0 = 5/9$, is by no means

indicated formally in Fig. 2; however, at $A_0 > 0.5$ the wave breaks at distances that do not exceed its length.

In the first series of experiments, the dimensionless depth of the trough was relatively small ($A_0 = 0.3$). The wave transformation is illustrated in Fig. 3 for different times.

The process of shock-wave formation and evolution qualitatively proceeds in accordance with predictions of weakly nonlinear theory [7, 9]. The shock wave begins to form within about 95 s in accordance with (8), but the initial stage is not very evident in Fig. 3. By about 200 s, the discontinuity in the wave is completely formed, and then the wave begins to decay in amplitude (Fig. 4).

As the amplitude increases, the nonlinear effects manifest themselves at smaller times and a new effect appears: the formation of the reflected wave from discontinuity in a running wave. Figure 5 illustrates this for $A_0 = 0.6$. The reflected wave has small amplitude and a large length comparable to the pulse length. The

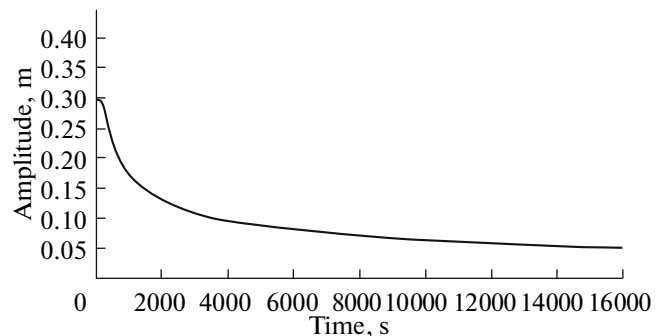


Fig. 4. Wave amplitude as a function of time ($A_0 = 0.3$).

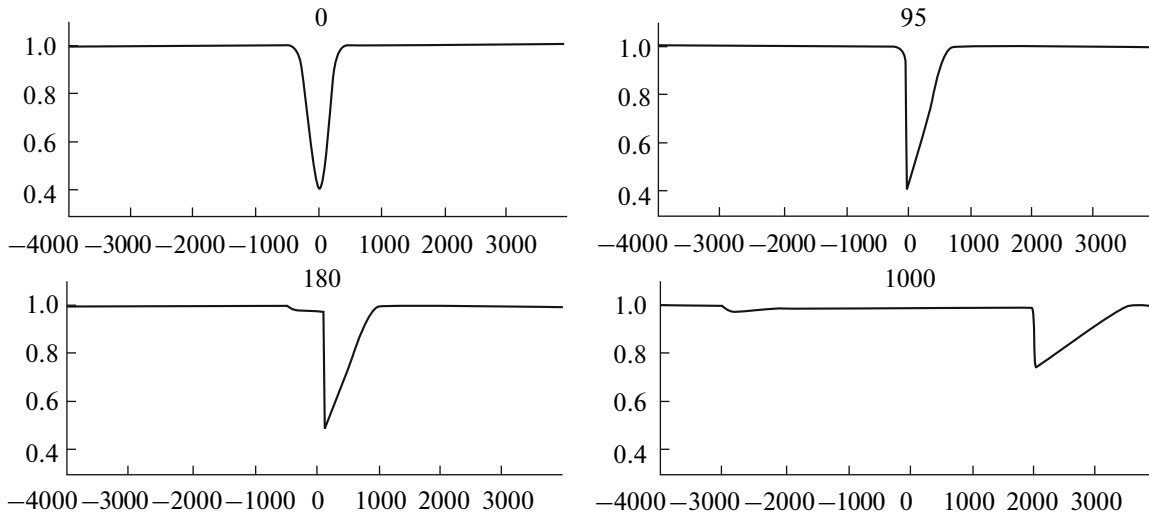


Fig. 5. Formation of the shock wave and the generation of the wave reflected from discontinuity ($A_0 = 0.6$).

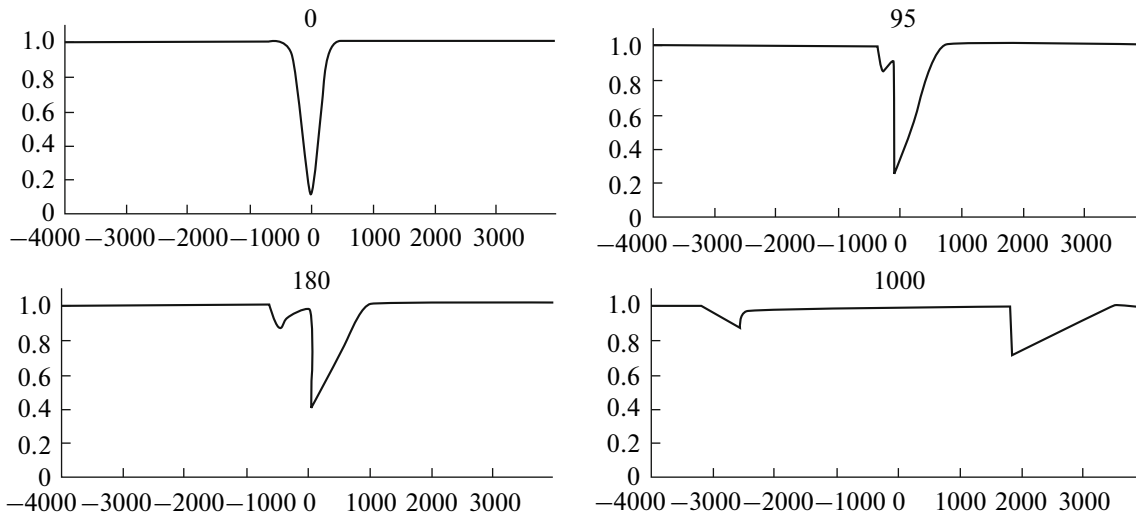


Fig. 6. Evolution of a strongly nonlinear shock wave ($A_0 = 0.9$).

origin of the reflected wave is described in [9]; it is related to the fact that the shock front cannot be inscribed in the Riemann wave (2). For large ampli-

tudes ($A_0 > 5/9$), this discrepancy is most noticeable: the Riemann wave should travel to the left, while the shock wave should propagate to the right.

The reflection from discontinuity is even more noticeable for strongly nonlinear waves, and Fig. 6 shows the structure of the wave field with amplitude $A_0 = 0.9$. In this case the reflected wave also transforms into a shock wave. Because the velocity of particles in the toe is lower than the linear velocity, the discontinuity forms on the back slope of the reflected wave.

It is well known that a change in the bore amplitude in the framework of weakly nonlinear theory can be found using the rule of equal squares [7, 9]. Without presenting rather cumbersome transcendental equations for the amplitude of the shock wave (their awkwardness arises from the Gaussian form of the initial

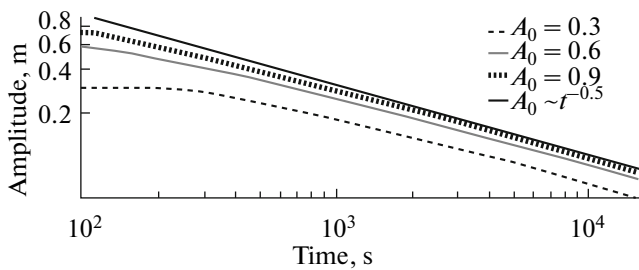


Fig. 7. Decay of the amplitude of the shock wave with time (initial amplitudes are shown by numbers).

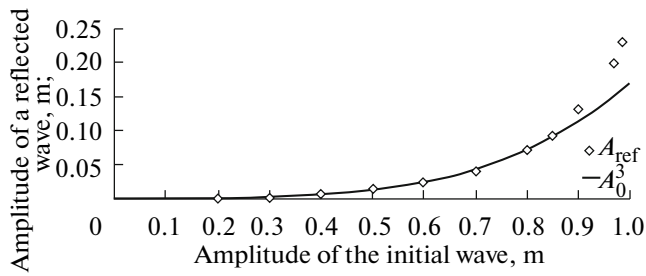


Fig. 8. Amplitude of the reflected wave arising from the formation of a shock wave versus the amplitude of the initial perturbation.

perturbation), we write an asymptotic expression valid in the final stage of shock-wave degeneration

$$A(t) \sim A_0 \sqrt{\frac{2T_{br}}{t}}. \tag{9}$$

The asymptotic curve given by (9) is depicted in Fig. 7 by a solid line. It describes changes in the ampli-

tude of the shock wave at large times well for both weakly nonlinear and strongly nonlinear waves.

The amplitude of the reflected wave versus the initial amplitude of the basic wave is shown in Fig. 8. According to the weakly nonlinear theory of acoustic shock waves in the third order of perturbation theory [9], the amplitude of the reflected wave is almost exactly equal to A_0^3 ; this asymptotic dependence is also shown in Fig. 8. As is seen, the asymptotic dependence works well not only for small-amplitude waves but also for large-amplitude waves ($A_0 \sim 0.8$), except for anomalously large amplitudes ($A_0 \sim 0.9-0.98$). One interesting case is the shape of the reflected wave, which remains a pulse and transforms at large times into a triangular pulse with a shock front in some sense mirror-reflected to the incident pulse. Note that the effect of reflection from the shock front, which was predicted in [9], was modeled in nonlinear transmission lines [3], where, however, dispersion played a role resulting in the reflection of a relatively high-frequency wave. In our calculations, the dispersion is zero and the

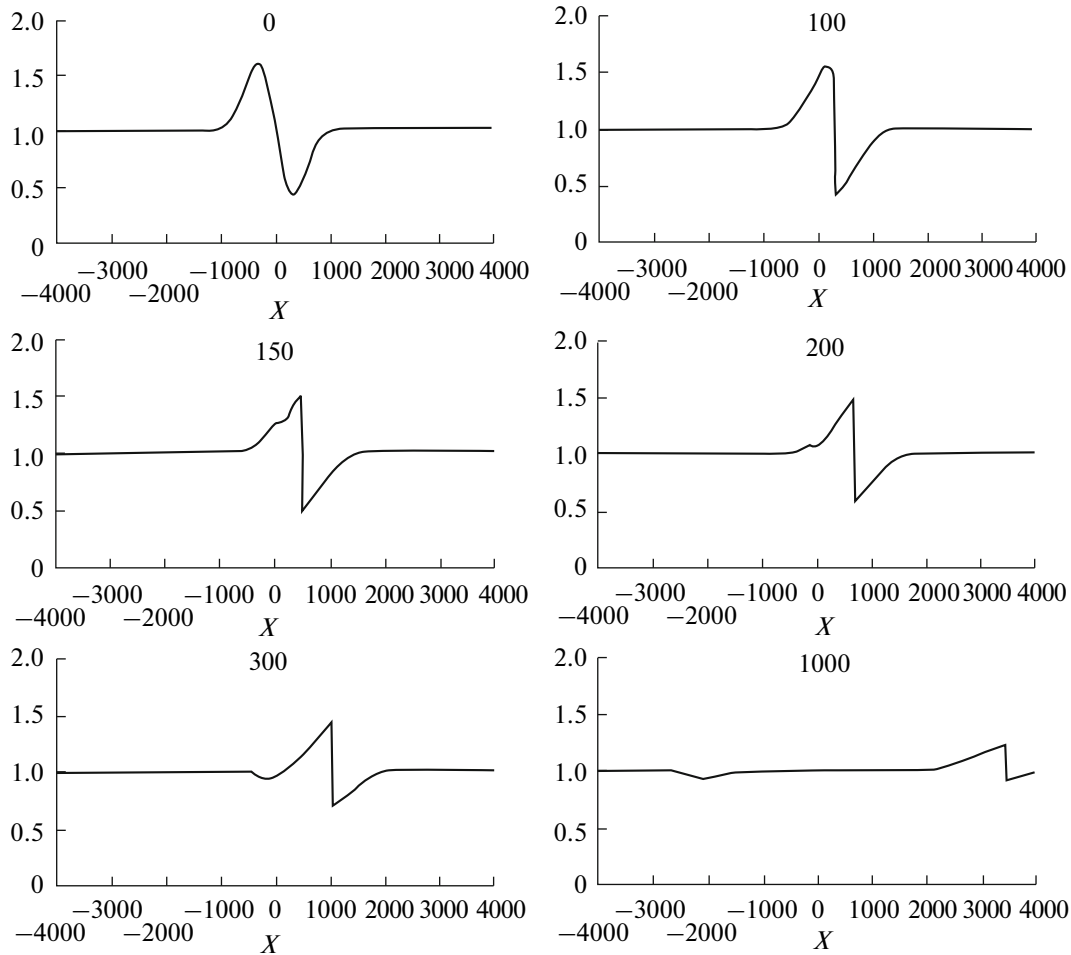


Fig. 9. Formation of the shock wave and generation of the reflected wave in the case of a sign-variable initial pulse ($A_0 = 0.6$ m).

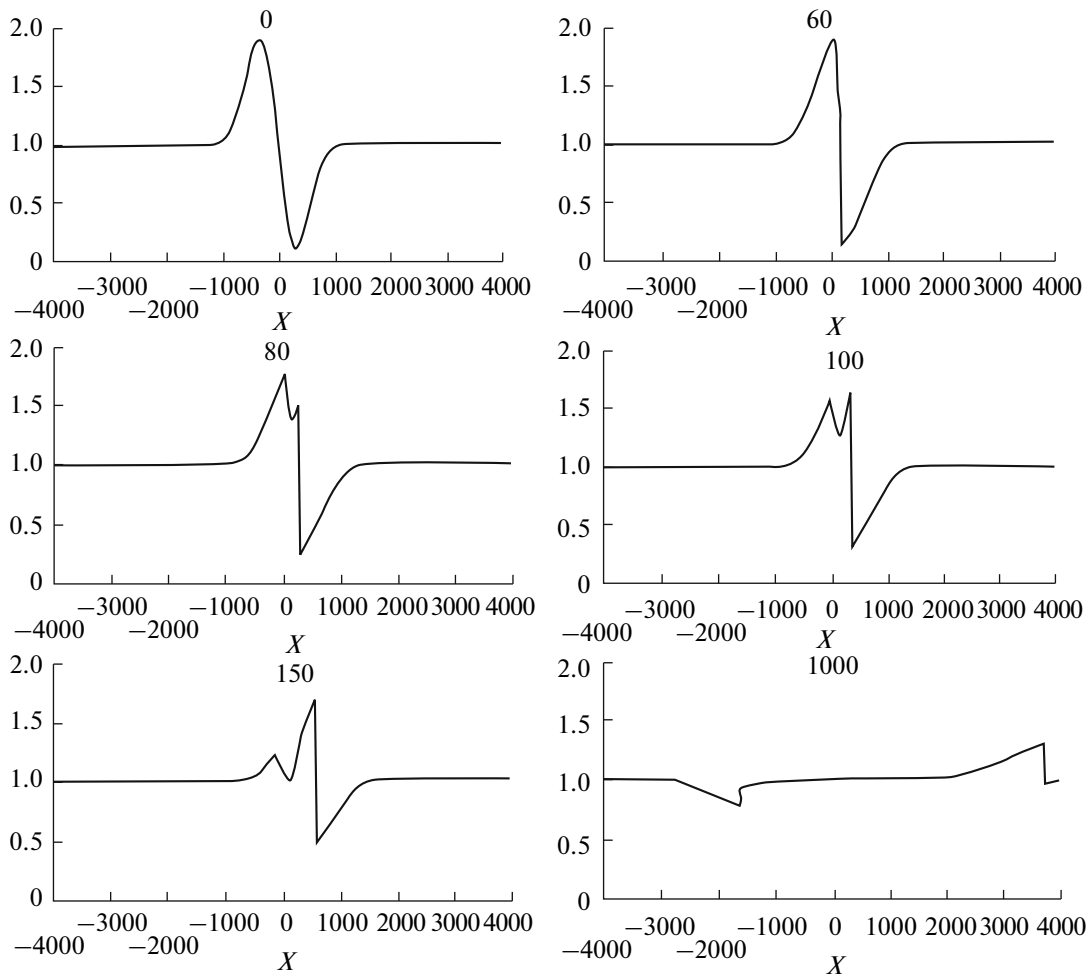


Fig. 10. Formation of the shock wave and generation of the reflected wave in the case of a sign-variable initial pulse ($A_0 = 0.9$ m).

reflected wave of large amplitude also becomes a shock wave, which is easily seen in Figs. 5 and 6.

To demonstrate the “difference” in the effect of nonlinearity on pulses of different polarities (crest and trough), we now consider a rightward-traveling sign-variable wave described by

$$H_0(x) = h \left[1 - B \exp\left(-\frac{x^2}{l^2}\right) \sin(kx) \right]. \quad (10)$$

In calculations, $h = 1$ m, $l = 1000$ m, $k = 5 \times 10^{-4} \text{ m}^{-1}$, and B was varied widely (0.1–10) so that the maximum departure of the profile from the equilibrium state $A_0 = B \times \text{Max}[\exp(-x^2/l^2)\sin(kx)]$ took values from 0 to h . The deformation of the wave with the initial amplitude $A_0 = 0.6$ m is shown in Fig. 9. As was noted before, the dynamics of the wave trough is strongly nonlinear and its part tends to move in the opposite direction. This property also manifests itself in a sign-variable wave. As a result, the pulse of negative polarity is separated from the wave and the reflected wave first interacts with the positive part of the basic wave. The shock wave propagating to the right becomes nonsymmetric

around the horizontal axis. These effects become even stronger for amplitudes $A_0 = 0.9$ (Fig. 10). In this case, the reflected wave rapidly turns into a shock wave and the basic wave eventually transforms into a positive shock triangle. This effect arises from the interaction of two shock waves of different polarities, one of which (hump) is more intense.

To sum up, we would like to emphasize several important conclusions inferred from the study we have conducted. The amplitude of the shock wave at large times decreases in proportion to $t^{-1/2}$, as is predicted by weakly nonlinear theory, despite the strong nonlinearities of the waves considered here. The front of the shock wave of negative polarity generates a reflected wave, which itself transforms into a shock wave at large times. Its amplitude is almost exactly equal to the cube of the initial amplitude over a wide range of the wave height, except for anomalously large heights. In the case of the sign-variable initial perturbation, the basic wave at long distances transforms into a shock wave of only positive polarity (hump).

ACKNOWLEDGMENTS

This work was supported in part by the Russian Foundation for Basic Research (project no. 11-05-0216), the Research Educational Center (project no. 02.740.11.0732) and ESF (8870, DoRa), the President of the Russian Federation (project no. MK-4378.2011.5), and by the program “Nonlinear Dynamics.”

REFERENCES

1. A. S. Arsen'ev and N. K. Shchelkovnikov, *Dynamics of Sea Long Waves* (Moscow State University, Moscow, 1991) [in Russian].
2. N. E. Vol'tsinger, K. A. Klevannyi, and E. N. Pelinovsky, *Longwave Dynamics of Coastal Zones* (Gidrometeoizdat, Leningrad, 1989) [in Russian].
3. K. I. Volyak, A. S. Gorshkov, and O. V. Rudenko, “On the Emergence of Back Waves in Homogeneous Nonlinear Media,” *Vestnik MGU: Ser. Fiz. Astron.*, No. 1, 32–36, (1975).
4. S. N. Gurbatov, A. I. Malakhov, and A. I. Saichev, *Nonlinear Random Waves in Dispersion-Free Media* (Nauka, Moscow, 1990) [in Russian].
5. I. I. Didenkulova, N. Zahibo, A. A. Kurkin, and E. N. Pelinovsky, “Steepness and Spectrum of a Nonlinearly Deformed Wave on Shallow Waters,” *Izv. Atmos. Ocean. Phys.* **42** (6), 773–776 (2006).
6. S. Nakamura, “On a Hydraulic Bore and Application of the Its Studying Results to the Problem of Tsunami Wave Emergence and Propagation,” in *Transactions of the Sakhalin Complex Scientific Research Institute* (SakhCRI, Yuzhno-Sakhalinks, 1973), No. 32, pp. 129–151.
7. E. N. Pelinovsky, *Nonlinear Dynamics of Tsunami Waves* (Institute of Applied Physics of USSR Acad. Sci., Gor'kii, 1982) [in Russian].
8. E. N. Pelinovsky, and E. N. Troshina, “Propagation of Long Waves in Straits,” *Phys. Oceanogr.* **5** (1), 43–48 (1994).
9. O. Rudenko and S. Soluyan, *Theoretical Foundations of Nonlinear Acoustics* (Nauka, Moscow, 1975) [in Russian].
10. J. Stokes, *Water Waves* (Wiley-Interscience, New York, 1957).
11. V. V. Shuleikin, *Marine Physics* (Nauka, Moscow, 1968) [in Russian].
12. J.-G. Caputo and Y. A. Stepanyants, “Bore Formation, Evolution, and Disintegration into Solitons in Shallow Inhomogeneous Channels,” *Nonlin. Processes Geophys.* **10** (4–5), 407–424 (2003).
13. R. J. LeVeque, *Finite-Volume Methods for Hyperbolic Problems* (Cambridge University Press, Cambridge, 2004).
14. P. L. Roe, “Approximate Riemann Solvers, Parameter Vectors, and Difference Schemes” *J. Comput. Phys.* **43** (2) 357–372 (1984).
15. Y. Tsuji, T. Yanuma, I. Murata, and C. Fujiwara, “Tsunami Ascending in Rivers as an Undular Bore,” *Nat. Hazards* **4**, 257–266 (1991).
16. N. Zahibo, E. Pelinovsky, T. Talipova, A. Kozelkov, and A. Kurkin, “Analytical and Numerical Study of Nonlinear Effects at Tsunami Modelling,” *Appl. Math. Comput.* **174** (2), 795–809 (2006).
17. N. Zahibo, I. Didenkulova, A. Kurkin, and E. Pelinovsky, “Steepness and Spectrum of Nonlinear Deformed Shallow Water,” *Ocean Eng.* **35** (1), 47–52 (2008).
18. Y. H. Wu and J.-W. Tian, “Mathematical Analysis of Long-Wave Breaking on Open Channels with Bottom Friction,” *Ocean Eng.* **26** (2), 187–201.